

---

# Continuous Monte Carlo Graph Search

---

Kalle Kujanpää<sup>1\*</sup>, Amin Babadi<sup>2\*</sup>, Yi Zhao<sup>2</sup>,  
Juho Kannala<sup>1</sup>, Alexander Ilin<sup>1</sup>, Joni Pajarinen<sup>2</sup>

\*Equal contribution

<sup>1</sup>Department of Computer Science, Aalto University

<sup>2</sup>Department of Electrical Engineering and Automation, Aalto University

## Abstract

In many complex sequential decision-making tasks, online planning is crucial for high performance. For efficient online planning, Monte Carlo Tree Search (MCTS) employs a principled mechanism for trading off exploration for exploitation. MCTS outperforms comparison methods in many discrete decision-making domains such as Go, Chess, and Shogi. Following, extensions of MCTS to continuous domains have been proposed. However, the inherent high branching factor and the resulting explosion of search tree size are limiting existing methods. To address this problem, we propose Continuous Monte Carlo Graph Search (CMCGS), a novel extension of MCTS to online planning in environments with continuous state and action spaces. CMCGS takes advantage of the insight that, during planning, sharing the same action policy between several states can yield high performance. To implement this idea, at each time step, CMCGS clusters similar states into a limited number of stochastic action bandit nodes, which produce a layered directed graph instead of an MCTS search tree. Experimental evaluation shows that CMCGS outperforms comparable planning methods in several complex continuous DeepMind Control Suite benchmarks and a 2D navigation task with limited sample budgets. Furthermore, CMCGS can be parallelized to scale up and it outperforms the Cross-Entropy Method (CEM) in continuous control with learned dynamics models.

## 1 Introduction

Monte Carlo Tree Search (MCTS) is a well-known online planning algorithm for solving the decision-making problem in discrete action spaces [12, 13]. MCTS achieves super-human performance in various domains such as Atari, Go, Chess, and Shogi [53] when a learned transition model is available. Recent research has therefore tried to extend MCTS to environments with continuous state and action spaces [23, 49, 36, 34, 32].

However, current MCTS approaches for continuous states and actions are limited [9, 11, 49, 32]. MCTS approaches that build the search tree by discretizing the action space or otherwise limiting the growth of the tree, such as progressive widening approaches [9, 11], do not scale up well to high-dimensional action spaces and complex problems due to the search space increasing exponentially with the planning horizon and action dimensionality, and they often require domain-specific knowledge to perform well [7, 65]. To alleviate this problem, learning-based approaches [49, 32] reduce the required planning horizon when a sufficiently large number of training samples is available but do not solve the underlying problem of increasing search space size.

To solve the search space explosion problem in MCTS-based planning, this paper presents Continuous Monte Carlo Graph Search (CMCGS), a novel extension of MCTS to the continuous control problem. Similarly to MCTS, CMCGS employs an iterative mechanism for building a search graph that yields the next action to execute. At each iteration, a series of operators is used to grow the search graph

and update the information stored in the graph nodes. CMCGS uses state clustering and Gaussian action bandits to deal with challenges posed by continuous states and actions.

Our experiments show that CMCGS outperforms strong planning baselines in several challenging benchmarks given limited interaction with the environment, including high-dimensional environments from the DeepMind Control Suite (DMC) [61]. We also show that CMCGS can be efficiently parallelized to scale up and demonstrate its generality and robustness with learned dynamics models in high-dimensional visual benchmarks, where CMCGS outperforms the Cross-Entropy Method (CEM) [51, 63]. Moreover, CMCGS shows strong performance by being superior to CEM in environments that require complex exploration, and our algorithm also works well in difficult, high-dimensional environments with informative rewards.

## 2 Related Work

**Monte Carlo Tree Search** (MCTS), a decision-time planning method in discrete action spaces [12, 35, 7], is a core component of the success of the computer Go game [19, 55, 56]. MCTS also shows advantages in general game playing [17, 21, 2, 20]. Several recent works combine MCTS with a learned dynamic model lifting the requirement for access to a simulator [53, 64]. Other recent MCTS-based methods combine similar states reached via different trajectories, but only in the discrete setting [37, 14].

**Online planning in continuous action spaces.** In continuous action spaces, there can be an infinite number of actions, which significantly increases the size of the MCTS search tree and makes applying out-of-the-box MCTS infeasible. Instead, CEM is vastly used in the continuous action domain as an online planning method [50, 51, 63, 10, 22]. Many methods combine CEM with a value function or policy in different ways to improve its performance [44, 38, 6, 28, 25]. The main limitation of CEM compared to MCTS (and this work) is that CEM models the whole action trajectory using a single sampling distribution. This could be translated into the context of MCTS as using only one node at each layer of the search tree, and it can limit the exploration capabilities of CEM in environments where there are several ways of controlling the agent, for example, going around an obstacle using two different ways. Covariance Matrix Adaptation Evolution Strategy (CMA-ES) is an evolutionary gradient-free algorithm for black-box continuous optimization [26, 27]. Although it has not seen much use in continuous control due to its computational complexity and memory requirements, applying it as an alternative to CEM has been proposed [29, 43, 15].

**MCTS in continuous action spaces** Since the success of MCTS in discrete action spaces, several attempts have been made to adopt it in the continuous action domain. To mitigate the requirement of enumerating all actions as in the discrete case, several works use progressive widening to increase the number of child actions of a node as a function of its visitation frequency [13, 9, 11, 40]. The action space can be split into bins by factorizing across action dimensions [24, 58]. Together with a learned value function, policy, and transition model, this method can successfully control a humanoid character with 21 action dimensions [59]. Besides these, a line of work extends MCTS to continuous action space via Hierarchical Optimistic Optimization (HOO) [8, 42, 39, 48]. HOO hierarchically partitions the action space by building a binary tree to incrementally split the action space into smaller subspaces. VG-UCT relies on action value gradients to perform local policy improvement [36]. Furthermore, several works grow the search tree based on sampling. Kernel regression can be used to generalize the value estimation, and thus limit the number of actions sampled per node [65]. The main difference to prior work is that we represent the search space as a graph instead of a tree and cluster similar states into search nodes to improve the performance with limited search budgets.

There are also learning-based approaches that represent the policy using a neural network and sample from it when expanding the tree [1, 32]. By leveraging the learned policy, these methods achieve promising performance with limited search budgets. However, we focus only on the core search component and leave comparisons with learning-based methods to future work.

## 3 Preliminaries

Planning and search is arguably the most classic approach for optimal control [16, 41, 59]. The idea of this approach is to start with a (rough) estimation of the action trajectory and gradually improve it through model-based simulation of the environment. In the case of environments with complex

dynamics, this is usually done online by optimizing only a small part of the action trajectory at each step. Then, the first action of the optimized trajectory is returned as the result. After executing the action, the whole process is repeated, starting from the newly visited state. This process is also known as closed-loop control, or model-predictive control (MPC). MPC has been shown to be an effective approach for optimal control in complex real-time environments [52, 18, 4].

Monte Carlo Tree Search (MCTS) [12] is one of the most popular MPC algorithms in environments such as video games [46, 31] that require principled exploration. MCTS starts by initializing a single-node search tree using the current state  $s_t$  as the root and grows the tree in an iterative manner, where one node is added to the tree at each iteration. The iterative process of MCTS is comprised of the following four key steps [7]:

1. **Selection (Tree Policy):** In this step, the algorithm selects one of the tree nodes to be expanded next. This is done by starting from the root and navigating to a child node until a node with at least one unexpanded child is visited using a selection criterion, whose goal is to balance the exploration-exploitation trade-off.
2. **Expansion:** In this step, MCTS expands the search tree by adding a (randomly chosen) unvisited child to the selected node from the previous step.
3. **Simulation (Default Policy):** After expanding the selected node, the newly added node is evaluated using a trajectory of random actions and computing the return.
4. **Backup:** In the final step, the computed return is backed up through the navigated nodes, updating the statistics stored in each node.

## 4 Continuous Monte Carlo Graph Search

We propose an algorithm for continuous control called Continuous Monte Carlo Graph Search (CMCGS). We assume a discrete-time, discounted Markov Decision Process (MDP) with continuous states and actions. CMCGS is an iterative planning algorithm in which each iteration contains the same four steps as MCTS with an additional width expansion step (see Fig. 1). Instead of building a search tree, CMCGS performs a search on a layered graph in which each layer corresponds to one step of the underlying MDP. We assume that we have access to a dynamics model  $p(s_{t+1}, r_{t+1} | s_t, \mathbf{a}_t)$  that can either be an exact model of the environment or a learned approximation.

Each node  $q$  in the  $t$ -th layer of the CMCGS graph corresponds to a *cluster of states visited at timestep  $t$* . The node is characterized by its state distribution  $p_q(s_t)$  and policy  $\pi_q(\mathbf{a}_t)$ , which describe the states assigned to this cluster and the preferred actions taken from this cluster during CMCGS planning. Both distributions  $p_q(s)$  and  $\pi_q(\mathbf{a}_t)$  are modeled as Gaussian distributions with diagonal covariance matrices. The distributions are fitted to the data using the replay buffer collected during planning. The replay buffer contains tuples  $e = (s_t, \mathbf{a}_t, s_{t+1}, R, q)$ , where  $q$  is the node to which state  $s_t$  belongs and  $R$  is the observed trajectory return. We denote by  $\mathcal{D}_q$  all the tuples in the replay buffer that correspond to node  $q$  and by  $Q_t$  the set of nodes in layer  $t$ .

The search graph is initialized with  $d_{\text{init}}$  layers such that each layer contains only one node. The CMCGS algorithm then iterates the following steps (see Fig. 1 for a graphical illustration).

- (a) **Selection:** The selection mechanism is repeatedly applied to navigate through the search graph starting from the root node until a sink node (a node without children) or a terminal state of the MDP is reached (Fig. 1a). When navigating through the graph, we use an epsilon-greedy-inspired policy: with probability  $\epsilon$ , we sample an action from the node policy  $\pi_q(\mathbf{a})$  and with probability  $1 - \epsilon$ , we select one of the top actions in  $\mathcal{D}_q$  and modify it with small Gaussian noise.<sup>1</sup> The current state  $s_t$  is updated to  $s_{t+1}$  according to the dynamics model, and the node in the next layer is selected by maximizing the probability of the updated state according to the node distributions:

$$q \leftarrow \arg \max_{q \in Q_{t+1}} p_q(s_{t+1})$$

- (b) **Depth expansion:** If the last layer of the graph has collected enough experience (the number of samples is greater than threshold  $m$ ) and the maximum graph depth has not been reached, we add a new layer to the graph (Fig. 1b). The new layer initially contains a single node.

<sup>1</sup>This approach enables the agent to leverage past experience efficiently while exploring new options, leading to better performance on complex tasks.

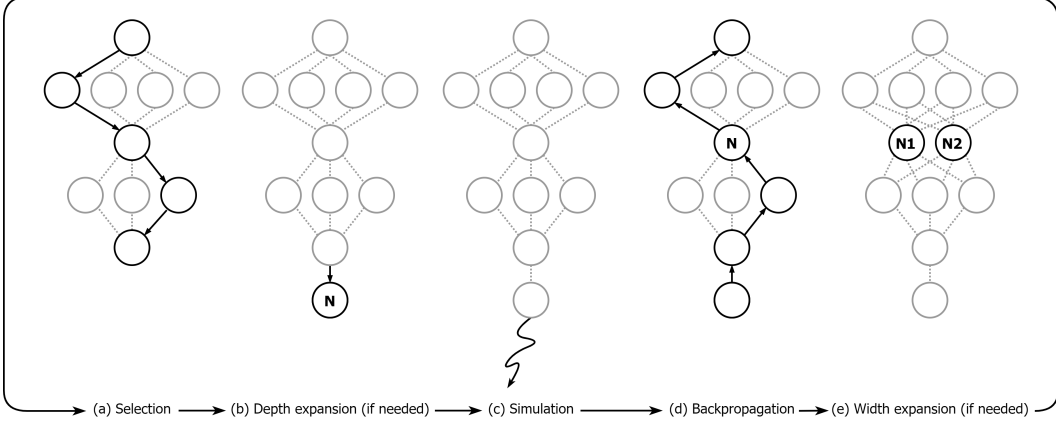


Figure 1: Core steps in one iteration of Continuous Monte Carlo Graph Search (CMCGS). a) Starting from the root node, the graph is navigated via action sampling and node selection until a sink node is reached. b) If there is enough experience collected in the final layer of the graph and the maximum depth has not been reached, a new layer containing a new node  $\mathbf{N}$  is initialized. c) A trajectory of random actions is simulated from the graph’s sink node to compute the accumulated reward. d) The computed accumulated reward is backed up through the selected nodes, updating their replay memories, policies, and state distributions. e) If a new cluster of experience data is found in a previous layer of the graph, all nodes in that layer are updated based on the new clustering information (in this example, the node  $\mathbf{N}$  is split into two new nodes  $\mathbf{N1}$  and  $\mathbf{N2}$ ).

- (c) **Simulation:** Similar to MCTS, we simulate a random trajectory using random actions starting from the sink node and compute the trajectory return  $R$  (Fig. 1c). The length of the rollout is controlled by parameter  $N_r$ , but the rollout is interrupted if a terminal state is encountered.
- (d) **Backup:** We traverse the search graph backward and update the node distributions  $p_q(s)$  and  $\pi_q(a)$  for all the nodes visited in the selection procedure (Fig. 1d). The means and variances of  $p_q(s)$  are updated by using the newly visited states. A node’s policy  $\pi_q(a)$  is updated if the node contains enough experience ( $|\mathcal{D}_q| > m/2$ ). The dimension means of  $\pi_q(a)$  are fitted to the highest-scoring (elite) experiences in  $\mathcal{D}_q$ , similarly to CEM. To update the dimension variances of  $\pi_q(a)$ , we adopt the Bayes’ rule by defining a conjugate prior (inverse gamma) on the variances, compute the posteriors using the elite samples, and select the posterior means as the variances.
- (e) **Width expansion:** The maximum desired number  $C_t$  of nodes in layer  $t$  is computed using a heuristic rule  $C_t = \min(n_{\max}, \lfloor n_t/m \rfloor)$  where  $n_t$  is the number of transitions collected at timestep  $t$ ,  $m$  a threshold hyperparameter, and  $n_{\max}$  is the hard limit on the nodes. If the current number of nodes in layer  $t$  is smaller than  $C_t$ , we attempt to cluster the states visited at timestep  $t$  into  $|Q_t| + 1$  clusters. We use Agglomerative Clustering with Ward linkage in our experiments due to its fast running time with the amounts of data used in our work [45, 62]. Using Euclidean distance as a metric is feasible both in low-dimensional state spaces and learned latent spaces. The clustering is approved if each cluster contains at least  $m/2$  states. Then, a new node is added to the layer (Fig. 1e), all experience tuples in the replay buffer are re-assigned to the corresponding nodes, and the state and action distributions of the affected nodes are updated. Otherwise, no new node is created and clustering is attempted again when the layer has collected  $m/2$  new samples.

When the simulation budget has been exhausted, the agent’s next action is determined by the experience stored at the root node. When the search has access to a deterministic environment simulator, the first action of the trajectory with the highest return is chosen. When searching with a learned dynamics model or the environment is stochastic, the average of the top actions in the replay memory of the root node is returned to prevent the exploitation of model inaccuracies or individual samples. Each of the five steps of CMCGS can be performed efficiently using batch operations, making it possible to collect multiple trajectories in parallel. The pseudocode of the CMCGS algorithm is shown in Algorithm 1.

---

**Algorithm 1** Continuous Monte Carlo Graph Search

---

```
1: function CMCGS( $s_0$ )
2:   Initialize the search graph with one node per layer and  $q_{\text{root}}$  as the root node.
3:   while within computational budget do
4:      $\tau, R, s_d \leftarrow \text{GRAPHPOLICY}(s_0, q_{\text{root}})$   $\triangleright \tau \leftarrow \{\langle s_t, \mathbf{a}_t, s_{t+1}, q_t \rangle\}_{t=0}^{d-1}$ 
5:     if  $s_d$  is not terminal then
6:        $R \leftarrow R + \text{RANDOMROLLOUT}(s_d)$ 
7:        $\text{BACKUP}(\tau, R)$ 
8:   return best action found in the replay memory of the root node  $q_{\text{root}}$ 
9: function GRAPHPOLICY( $s, q$ )
10:   $\tau \leftarrow \emptyset$ 
11:   $R \leftarrow 0$ 
12:   $\phi \leftarrow \begin{cases} 1, & \text{if } \mathcal{U}(0, 1) < \epsilon \\ 0, & \text{otherwise} \end{cases}$ 
13:  while  $s$  is not terminal and not visited all graph layers do
14:     $\mathbf{a} \sim \phi \pi_q(\mathbf{a}) + (1 - \phi) \pi_{q, \text{greedy}}(\mathbf{a})$ 
15:    Apply action  $\mathbf{a}$  and observe new state  $s'$  and reward  $r$ 
16:     $\tau \leftarrow \tau \cup \{\langle s, \mathbf{a}, s', q \rangle\}$ 
17:     $R \leftarrow R + r$ 
18:    if  $s'$  is not terminal and we are visiting the last layer of the graph then
19:      Try adding a new layer with one node to the graph.
20:    if  $s'$  is terminal or we are visiting the last layer of the graph then
21:      break
22:     $q \leftarrow \arg \max_{q \in Q_{t+1}} p_q(s')$ 
23:     $s \leftarrow s'$ 
24:  return  $\tau, R, s$ 
25: function BACKUP( $\tau, R$ )
26:  for each  $\langle s_t, \mathbf{a}_t, s_{t+1}, q_t \rangle \in \tau$  do
27:    Store the new experience  $\langle s_t, \mathbf{a}_t, R, s_{t+1}, q_t \rangle$  in replay buffer
28:    Compute  $C_t$ , the desired number of clusters in layer  $t$ 
29:    if there are fewer than  $C_t$  clusters in layer  $t$  then
30:      Try to cluster states  $\{s_t\}$  in layer  $t$  into  $|Q_t| + 1$  clusters
31:      if clustering was successful then
32:        Replace nodes in layer  $t$  with the new nodes
33:        Estimate node state distributions  $p_q(s)$  and policies  $\pi_q(\mathbf{a})$ 
34:      if no new cluster has been found in layer  $t$  then
35:        Update  $p_q(s)$  and  $\pi_q(\mathbf{a})$  of the visited node  $q_t$ 
```

---

## 5 Experiments

We ran three sets of experiments to evaluate the performance, generality, and robustness of CMCGS. First, we present a motivating example where CEM fails due to its inability to explore properly in an environment where a multimodal representation of the action distribution is useful. Second, we evaluate CMCGS in continuous control tasks with limited sample budgets to demonstrate that it outperforms relevant baselines in a variety of tasks with different levels of exploration required. Finally, we demonstrate that CMCGS can be parallelized and can successfully utilize learned models for large-scale planning in complex tasks by showing that it achieves significantly better planning performance than CEM in image-based continuous control environments.

### 5.1 Toy Environment

We design a toy environment where the agent samples  $N$  actions  $a_1, \dots, a_N$  sequentially and receives a basic reward of  $r = 0.5$  if the absolute value of each action is greater than 1. An additional reward

Table 1: The success rates of achieving the small and large rewards and the average rewards achieved by different algorithms in the toy environment plus-minus two standard errors.

Method	$r \geq 0.5$	$r = 1.0$	Average Reward
CMCGS	<b>1.00</b>	<b>0.97</b>	<b>0.983</b> $\pm$ 0.004
Random shooting	<b>1.00</b>	0.89	0.943 $\pm$ 0.010
CEM	0.74	0.57	0.655 $\pm$ 0.028

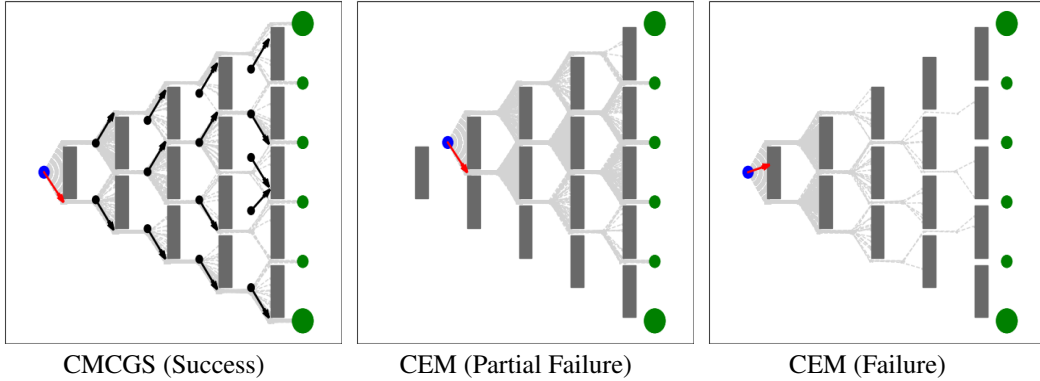


Figure 2: An illustration of exploration in the toy environment. The agent, the chosen action, the explored trajectories, and the different-sized rewards are represented by the blue dot, red arrow, grey dashed lines, and green dots, respectively. The search nodes of CMCGS and the corresponding state and action means are illustrated with black dots and arrows. The left image illustrates how CMCGS explores with state-dependent policies. In the other pictures, we see how CEM fails in the environment. CEM can either fail to discover the large reward and choose a suboptimal action (center), or completely fail to handle the required multimodality of the environment (right).

of 0.5 is given if the sign of all actions is the same. The reward is formalized as

$$r = \begin{cases} 0.5, & \text{if } \forall i \in \{1, \dots, N\} : |a_i| > 1 \\ 1, & \text{if } \forall i \in \{1, \dots, N\} : |a_i| > 1 \wedge \forall i \in \{2, \dots, N\} : \text{sgn}(a_i) = \text{sgn}(a_1) \end{cases}$$

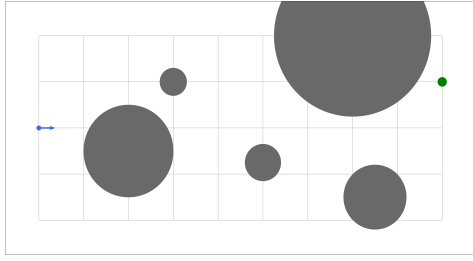
All action bandits are initialized to  $\mathcal{N}(0, 1)$ . Finding the basic reward of  $r = 0.5$  within the given search budget is easy, but performing principled exploration to find the additional component is a challenge. Furthermore, being able to represent complex multimodal action distributions is a valuable asset in this environment. In practice, we let  $N = 5$  and compare our method to random shooting and CEM. The results are plotted in Table 1 and the agents' behavior is illustrated in Fig. 2. The results show that CEM struggles to explore the environment properly, and the CMCGS outperforms random shooting due to directed exploration. What is more, CEM sometimes fails to receive the basic reward of 0.5 due to the inability to represent the multimodal action distribution natural to this problem.

## 5.2 Continuous Control with Limited Interaction

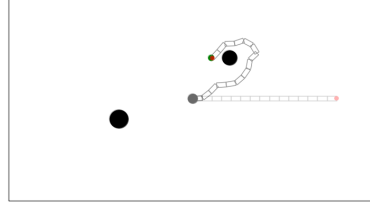
Second, we compare CMCGS against the strong planning algorithms (1) Monte Carlo Tree Search with Progressive Widening (MCTS-PW) [9, 11], (2) CEM [50], and (3) CMA-ES [27] to demonstrate the power of CMCGS in continuous control tasks when the number of environment interactions is a bottleneck. This can be the case in, for instance, real-life robotics or when a computationally very intensive and accurate simulator is used. In these tasks, we evaluate the planning performance of the algorithms on real dynamics. We also include standard random shooting as a baseline.

The environments we use in these experiments include:

1. **2D Navigation:** We developed an environment for control of a particle such that it tries to reach the goal (shown in green in Fig. 3a) without colliding with the obstacles. We used two variations of this environment, one with circular and another with rectangular obstacles. In these environments, a new action is applied whenever the particle reaches a vertical gray



(a) 2D navigation task using circular obstacles (*2d-navigation-circles*).



(b) 2D reacher task using 15-linked arm (*2d-reacher-fifteen-poles*).

Figure 3: Custom environments used in the experiments.

line. The main challenge in these environments is that the agent has to explore to find the green reward and avoid colliding with the obstacles.

2. **2D Reacher:** Since *2D Navigation* environments only have 1 Degree of Freedom (DOF), we also developed a variation of the classic reacher task for a 2D multi-link arm. In this environment, only a sparse binary reward is used for reaching the goal (shown in green in Fig. 3b), and there are obstacles (shown in black) that block the path. We use 15- and 30-linked arms to evaluate the scalability of CMCGS to high-dimensional action spaces. The 15-link variation is shown in Fig. 3b.
3. **DeepMind Control Suite:** We also used several popular environments provided by DeepMind Control Suite [60] in our experiments. These environments pose a wide range of challenges for continuous control with low- and high-dimensional states and actions. In this part of the evaluation, we use proprioceptive observations.

We evaluate CMCGS and the baselines CEM, MCTS-PW, CMA-ES, and random shooting using different simulation budgets per control timestep. For each budget, we used 400 random seeds for 2D navigation tasks, 200 for 2D reacher tasks, and 100 for DMC tasks. All experiments used the same set of hyperparameters (see supplementary material).

We plot the means of the episode returns in Fig. 4 and the complete results in Fig. 5. The plots show the mean plus-minus two standard errors. CMCGS demonstrates the best performance compared to the baselines. In the four 2D environments that test exploration, CMCGS is the best, and it is also the best overall in the DMC environments where exploration is less challenging. CMCGS is highly robust to the different sizes of simulation budgets and achieves the best mean performance in the DMC environments at every simulation budget. CEM uses a single bandit for each time step, MCTS-PW creates a search tree that grows with each time step, and CMA-ES creates a distribution over all time steps with temporal correlations but assumes a uni-modal distribution and does not divide planning into different nodes for different state distributions [50, 47]. Therefore, CEM and CMA-ES perform poorly in tasks that require strong exploration, and MCTS-PW performs poorly in tasks that require taking advantage of informative rewards. CMCGS uses several nodes, similar to MCTS, for different state distributions but limits the number of nodes at each time step allowing for strong exploration while still taking advantage of informative rewards.

CMA-ES outperforms CMCGS in the *cheetah* and *walker* environments, most likely due to being able to take advantage of the informative rewards and the covariance matrix that takes correlations

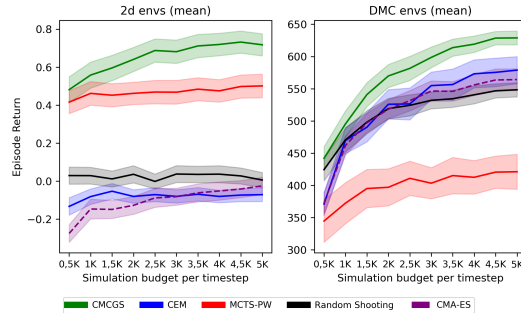


Figure 4: The mean episode returns averaged over (left) the custom 2D environments that test exploration and (right) the environments from DeepMind Control Suite.

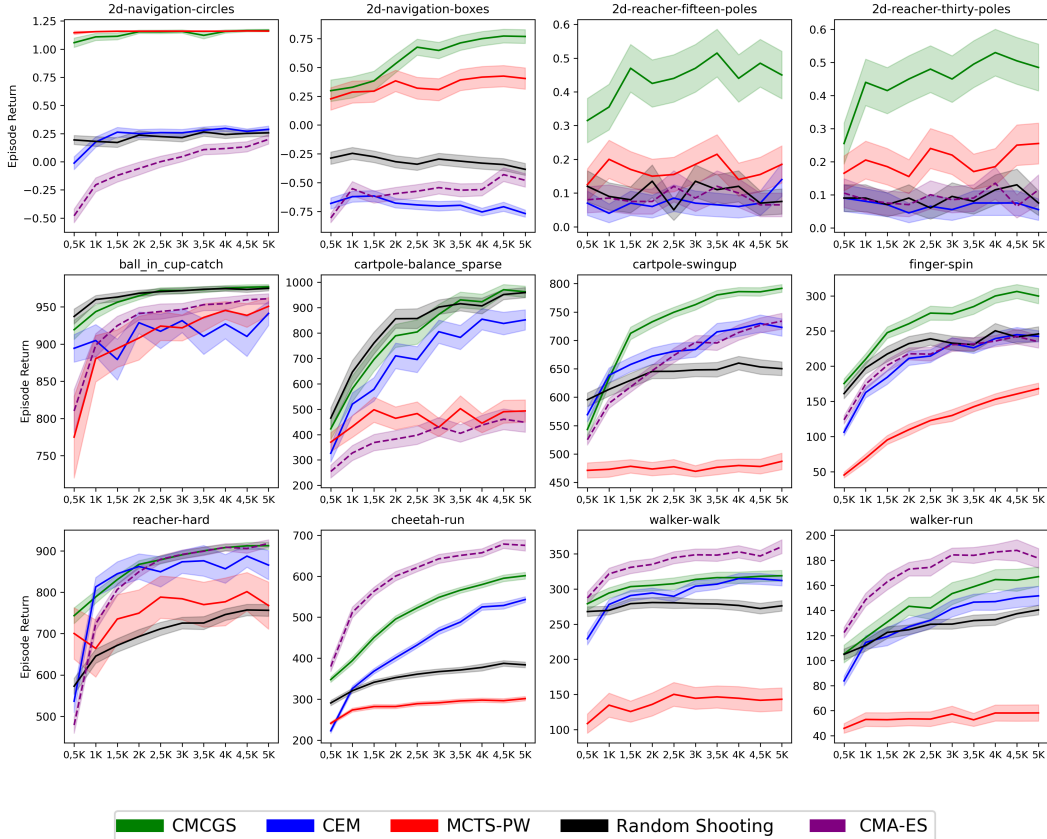


Figure 5: Reward plots for different simulation budgets per timestep.  $2d$ - $X$  environments (first row) have been developed by the authors to test exploration. The rest are from DeepMind Control Suite with proprioceptive observations. The proposed CMC GS shows the best performance overall.

over all time steps into account. However, it is inferior to CEM in many environments despite CEM assuming a much simpler sampling distribution without any temporal correlations, which was also observed in Duan et al. [15]. MCTS-PW performs very well in low-dimensional and sparse reward environments such as the 2d navigation environments and *ball\_in\_cup-catch*, but high action dimensionality makes it struggle, especially in the *walker* environments. We observe that the progressive widening strategy is not enough to make MCTS handle long planning horizons with the search space growing exponentially. For the complete results, please see the supplementary material.

### 5.3 Large-Scale CMC GS with Learned Models

We demonstrate the generality of CMC GS by evaluating it with learned dynamics models in high-dimensional environments and comparing it to CEM. For evaluation, we use pixel-based environments from the DeepMind Control Suite [60] and PlaNet [22] as the underlying algorithm for learning the dynamics model. We use an open-sourced implementation of PlaNet and pre-trained models by Arulkumaran [3] and replace CEM with CMC GS as the planner during evaluation. PlaNet has an encoder that learns a latent representation from pixels, and CMC GS performs planning and clustering in this learned latent space.

We copy the hyperparameters for CEM from the original paper [22] and perform equally many simulator interactions with CMC GS. We let CMC GS collect 400 trajectories in parallel, and as a result, the running times of the algorithms are of the same magnitude. The mean episode returns in Table 2 show that CMC GS outperforms CEM in six of the seven environments, and is significantly better overall. CMC GS does not exploit the model inaccuracies, which makes it a robust and general planning algorithm for high-dimensional continuous control tasks.



Table 2: The average rewards attained in the DMC environments with image observations using learned PlaNet dynamics models for planning with CEM and CMCGS as the planning algorithms plus-minus two standard errors.

Environment	CEM	CMCGS
Ball-in-Cup Catch	713.4 $\pm$ 31.6	<b>840.1</b> $\pm$ 18.7
Cartpole Balance	<b>996.7</b> $\pm$ 0.1	995.0 $\pm$ 0.1
Cartpole Swingup	763.1 $\pm$ 4.5	<b>859.0</b> $\pm$ 0.5
Cheetah Run	556.5 $\pm$ 8.5	<b>640.3</b> $\pm$ 17.8
Finger Spin	651.1 $\pm$ 9.5	<b>837.9</b> $\pm$ 3.0
Reacher Easy	828.4 $\pm$ 46.1	<b>845.7</b> $\pm$ 44.5
Walker Walk	863.1 $\pm$ 21.3	<b>952.4</b> $\pm$ 4.0
Mean	767.5 $\pm$ 23.2	<b>852.9</b> $\pm$ 19.5

## 6 Limitations and Future Work

In this section, we explain the main limitations of the proposed algorithm, CMCGS, and how they could be addressed in future work.

**Bootstrapping:** In our current implementation, CMCGS builds the search graph from scratch at each timestep. Model-predictive control can benefit from using the best solution from previous timestep(s) to bias the optimization process towards more promising trajectories if the model is accurate [30, 5]. In CMCGS, this could be done by biasing the mean of the action policies of the search nodes towards the old best actions. A more trivial approach would be to simply inject the old best trajectory into the replay memory of the search nodes.

**Learning:** MCTS can benefit from learned value functions, policy priors, or rollout policies that have been trained using imitation learning from pre-existing datasets [54, 33, 57]. We believe that this could improve the performance of CMCGS.

**Arbitrary graph structures:** Currently, CMCGS uses a layered directed acyclic graph to represent the state space, which does not allow the search graph to re-use previous experience in environments where the agent can navigate back and forth between different states (such as searching through a maze). This limitation could be lifted by allowing the algorithm to build arbitrary graph structures (such as complete graphs) to better utilize the structure of the state space during planning.

## 7 Conclusion

In this paper, we proposed Continuous Monte Carlo Graph Search (CMCGS), an extension of the popular MCTS algorithm for solving decision-making problems with high-dimensional continuous state and action spaces. CMCGS builds up on the observation that different regions of the state space ask for different action bandits for estimating the reward and representing the action distribution. Based on this observation, CMCGS builds a layered search graph where, at each layer, the visited states are clustered into several stochastic action bandit nodes, which allows CMCGS to solve complex high-dimensional continuous control problems efficiently. CMCGS outperforms MCTS-PW, CEM, and CMA-ES in several complex continuous control environments such as DeepMind Control Suite benchmarks. Experiments in sparse-reward custom environments indicate that CMCGS has significantly better exploration capabilities than the evaluated baselines, especially given a high-dimensional action space.

CMCGS can be efficiently parallelized, which makes the algorithm practically relevant also for large-scale planning. Our experiments with the learned PlaNet dynamics models show that CMCGS can be scaled up to be competitive with CEM as a planning component of general model-based reinforcement learning algorithms that learn from pixels, where the number of environment interactions is not a limiting factor and exploration is less important. We believe that the proposed CMCGS algorithm could be a building block for a new family of Monte Carlo methods applied to decision-making problems with continuous action spaces.

## Acknowledgments and Disclosure of Funding

We acknowledge the computational resources provided by the Aalto Science-IT project and CSC, Finnish IT Center for Science. The work was funded by Research Council of Finland (aka Academy of Finland) within the Flagship Programme, Finnish Center for Artificial Intelligence (FCAI). J. Pajarinen was partly supported by Research Council of Finland (aka Academy of Finland) (345521).

## References

- [1] Zaheen Ahmad, Levi Lelis, and Michael Bowling. Marginal utility for planning in continuous or large discrete action spaces. *Advances in Neural Information Processing Systems*, 33: 1937–1946, 2020.
- [2] Thomas Anthony, Zheng Tian, and David Barber. Thinking fast and slow with deep learning and tree search. *Advances in Neural Information Processing Systems*, 30, 2017.
- [3] Kai Arulkumaran. Pytorch implementation of planet: A deep planning network for reinforcement learning. <https://github.com/Kaixhin/PlaNet>, 2019.
- [4] Amin Babadi, Kouros Naderi, and Perttu Hämäläinen. Intelligent middle-level game control. In *Proceedings of IEEE Conference on Computational Intelligence and Games (CIG)*, pages 25–32. IEEE, 2018.
- [5] Mohak Bhardwaj, Sanjiban Choudhury, and Byron Boots. Blending mpc & value function approximation for efficient reinforcement learning. *arXiv preprint arXiv:2012.05909*, 2020.
- [6] Mohak Bhardwaj, Ankur Handa, Dieter Fox, and Byron Boots. Information theoretic model predictive q-learning. In *Learning for Dynamics and Control*, pages 840–850. PMLR, 2020.
- [7] Cameron B Browne, Edward Powley, Daniel Whitehouse, Simon M Lucas, Peter I Cowling, Philipp Rohlfshagen, Stephen Tavener, Diego Perez, Spyridon Samothrakis, and Simon Colton. A survey of monte carlo tree search methods. *IEEE Transactions on Computational Intelligence and AI in games*, 4(1):1–43, 2012.
- [8] Sébastien Bubeck, Gilles Stoltz, Csaba Szepesvári, and Rémi Munos. Online optimization in x-armed bandits. *Advances in Neural Information Processing Systems*, 21, 2008.
- [9] Guillaume M JB Chaslot, Mark HM Winands, H Jaap van den Herik, Jos WHM Uiterwijk, and Bruno Bouzy. Progressive strategies for monte-carlo tree search. *New Mathematics and Natural Computation*, 4(03):343–357, 2008.
- [10] Kurtland Chua, Roberto Calandra, Rowan McAllister, and Sergey Levine. Deep reinforcement learning in a handful of trials using probabilistic dynamics models. *Advances in neural information processing systems*, 31, 2018.
- [11] Adrien Couëtoux, Jean-Baptiste Hoock, Nataliya Sokolovska, Olivier Teytaud, and Nicolas Bonnard. Continuous upper confidence trees. In *International Conference on Learning and Intelligent Optimization*, pages 433–445. Springer, 2011.
- [12] Rémi Coulom. Efficient selectivity and backup operators in monte-carlo tree search. In *International conference on computers and games*, pages 72–83. Springer, 2006.
- [13] Rémi Coulom. Computing “elo ratings” of move patterns in the game of go. *ICGA journal*, 30(4):198–208, 2007.
- [14] Johannes Czech, Patrick Korus, and Kristian Kersting. Improving alphazero using monte-carlo graph search. In *Proceedings of the International Conference on Automated Planning and Scheduling*, volume 31, pages 103–111, 2021.
- [15] Yan Duan, Xi Chen, Rein Houthoofd, John Schulman, and Pieter Abbeel. Benchmarking deep reinforcement learning for continuous control. In *International conference on machine learning*, pages 1329–1338. PMLR, 2016.

- [16] Richard E Fikes and Nils J Nilsson. Strips: A new approach to the application of theorem proving to problem solving. *Artificial intelligence*, 2(3-4):189–208, 1971.
- [17] Hilmar Finnsson and Yngvi Björnsson. Simulation-based approach to general game playing. In *Aaai*, volume 8, pages 259–264, 2008.
- [18] Raluca D Gaina, Simon M Lucas, and Diego Pérez-Liébana. Population seeding techniques for rolling horizon evolution in general video game playing. In *Evolutionary Computation (CEC), 2017 IEEE Congress on*, pages 1956–1963. IEEE, 2017.
- [19] Sylvain Gelly and David Silver. Monte-carlo tree search and rapid action value estimation in computer go. *Artificial Intelligence*, 175(11):1856–1875, 2011.
- [20] Jean-Bastien Grill, Florent Altché, Yunhao Tang, Thomas Hubert, Michal Valko, Ioannis Antonoglou, and Rémi Munos. Monte-carlo tree search as regularized policy optimization. In *International Conference on Machine Learning*, pages 3769–3778. PMLR, 2020.
- [21] Xiaoxiao Guo, Satinder Singh, Honglak Lee, Richard L Lewis, and Xiaoshi Wang. Deep learning for real-time atari game play using offline monte-carlo tree search planning. *Advances in neural information processing systems*, 27, 2014.
- [22] Danijar Hafner, Timothy Lillicrap, Ian Fischer, Ruben Villegas, David Ha, Honglak Lee, and James Davidson. Learning latent dynamics for planning from pixels. In *International conference on machine learning*, pages 2555–2565. PMLR, 2019.
- [23] Perttu Hämäläinen, Sebastian Eriksson, Esa Tanskanen, Ville Kyrki, and Jaakko Lehtinen. Online motion synthesis using sequential monte carlo. *ACM Transactions on Graphics (TOG)*, 33(4):51, 2014.
- [24] Jessica B Hamrick, Abram L Friesen, Feryal Behbahani, Arthur Guez, Fabio Viola, Sims Witherspoon, Thomas Anthony, Lars Buesing, Petar Veličković, and Théophane Weber. On the role of planning in model-based deep reinforcement learning. *arXiv preprint arXiv:2011.04021*, 2020.
- [25] Nicklas Hansen, Xiaolong Wang, and Hao Su. Temporal difference learning for model predictive control. *arXiv preprint arXiv:2203.04955*, 2022.
- [26] Nikolaus Hansen and Andreas Ostermeier. Adapting arbitrary normal mutation distributions in evolution strategies: The covariance matrix adaptation. In *Proceedings of IEEE international conference on evolutionary computation*, pages 312–317. IEEE, 1996.
- [27] Nikolaus Hansen, Sibylle D Müller, and Petros Koumoutsakos. Reducing the time complexity of the derandomized evolution strategy with covariance matrix adaptation (cma-es). *Evolutionary computation*, 11(1):1–18, 2003.
- [28] Nathan Hatch and Byron Boots. The value of planning for infinite-horizon model predictive control. In *2021 IEEE International Conference on Robotics and Automation (ICRA)*, pages 7372–7378. IEEE, 2021.
- [29] Verena Heidrich-Meisner and Christian Igel. Uncertainty handling cma-es for reinforcement learning. In *Proceedings of the 11th Annual conference on Genetic and evolutionary computation*, pages 1211–1218, 2009.
- [30] Martin Herceg, CN Jones, and M Morari. Dominant speed factors of active set methods for fast mpc. *Optimal Control Applications and Methods*, 36(5):608–627, 2015.
- [31] Christoffer Holmgård, Michael Cerny Green, Antonios Liapis, and Julian Togelius. Automated playtesting with procedural personas through mcts with evolved heuristics. *IEEE Transactions on Games*, 11(4):352–362, 2018.
- [32] Thomas Hubert, Julian Schrittwieser, Ioannis Antonoglou, Mohammadamin Barekatain, Simon Schmitt, and David Silver. Learning and planning in complex action spaces. In *International Conference on Machine Learning*, pages 4476–4486. PMLR, 2021.

- [33] Bilal Kartal, Pablo Hernandez-Leal, and Matthew E Taylor. Action guidance with mcts for deep reinforcement learning. In *Proceedings of the AAAI conference on artificial intelligence and interactive digital entertainment*, volume 15, pages 153–159, 2019.
- [34] Beomjoon Kim, Kyungjae Lee, Sungbin Lim, Leslie Kaelbling, and Tomás Lozano-Pérez. Monte carlo tree search in continuous spaces using voronoi optimistic optimization with regret bounds. In *Proceedings of the AAAI Conference on Artificial Intelligence*, volume 34, pages 9916–9924, 2020.
- [35] Levente Kocsis and Csaba Szepesvári. Bandit based monte-carlo planning. In *European conference on machine learning*, pages 282–293. Springer, 2006.
- [36] Jongmin Lee, Wonseok Jeon, Geon-Hyeong Kim, and Kee-Eung Kim. Monte-carlo tree search in continuous action spaces with value gradients. In *Proceedings of the AAAI Conference on Artificial Intelligence*, volume 34, pages 4561–4568, 2020.
- [37] Edouard Leurent and Odalric-Ambrym Maillard. Monte-carlo graph search: the value of merging similar states. In *Asian Conference on Machine Learning*, pages 577–592. PMLR, 2020.
- [38] Kendall Lowrey, Aravind Rajeswaran, Sham Kakade, Emanuel Todorov, and Igor Mordatch. Plan online, learn offline: Efficient learning and exploration via model-based control. *arXiv preprint arXiv:1811.01848*, 2018.
- [39] Weichao Mao, Kaiqing Zhang, Qiaomin Xie, and Tamer Basar. Poly-hoot: Monte-carlo planning in continuous space mdps with non-asymptotic analysis. *Advances in Neural Information Processing Systems*, 33:4549–4559, 2020.
- [40] Thomas M Moerland, Joost Broekens, Aske Plaat, and Catholijn M Jonker. A0c: Alpha zero in continuous action space. *arXiv preprint arXiv:1805.09613*, 2018.
- [41] Igor Mordatch, Emanuel Todorov, and Zoran Popović. Discovery of complex behaviors through contact-invariant optimization. *ACM Transactions on Graphics (TOG)*, 31(4):1–8, 2012.
- [42] Rémi Munos et al. From bandits to monte-carlo tree search: The optimistic principle applied to optimization and planning. *Foundations and Trends® in Machine Learning*, 7(1):1–129, 2014.
- [43] Kourosh Naderi, Joose Rajamäki, and Perttu Hämäläinen. Discovering and synthesizing humanoid climbing movements. *ACM Transactions on Graphics (TOG)*, 36(4):43:1–43:11, July 2017. ISSN 0730-0301. doi: 10.1145/3072959.3073707. URL <http://doi.acm.org/10.1145/3072959.3073707>.
- [44] Rudy R Negenborn, Bart De Schutter, Marco A Wiering, and Hans Hellendoorn. Learning-based model predictive control for markov decision processes. *IFAC Proceedings Volumes*, 38(1): 354–359, 2005.
- [45] Fabian Pedregosa, Gaël Varoquaux, Alexandre Gramfort, Vincent Michel, Bertrand Thirion, Olivier Grisel, Mathieu Blondel, Peter Prettenhofer, Ron Weiss, Vincent Dubourg, et al. Scikit-learn: Machine learning in Python. *Journal of machine Learning research*, 12:2825–2830, 2011.
- [46] Diego Perez, Spyridon Samothrakis, and Simon Lucas. Knowledge-based fast evolutionary mcts for general video game playing. In *2014 IEEE Conference on Computational Intelligence and Games*, pages 1–8. IEEE, 2014.
- [47] Cristina Pinneri, Shambhuraj Sawant, Sebastian Blaes, Jan Achterhold, Joerg Stueckler, Michal Rolinek, and Georg Martius. Sample-efficient cross-entropy method for real-time planning. In *Conference on Robot Learning*, pages 1049–1065. PMLR, 2021.
- [48] Ricardo Quinteiro, Francisco S Melo, and Pedro A Santos. Limited depth bandit-based strategy for monte carlo planning in continuous action spaces. *arXiv preprint arXiv:2106.15594*, 2021.
- [49] Joose Julius Rajamäki and Perttu Hämäläinen. Continuous control monte carlo tree search informed by multiple experts. *IEEE transactions on visualization and computer graphics*, 2018.

- [50] Reuven Y Rubinstein. Optimization of computer simulation models with rare events. *European Journal of Operational Research*, 99(1):89–112, 1997.
- [51] Reuven Y Rubinstein and Dirk P Kroese. *The cross-entropy method: a unified approach to combinatorial optimization, Monte-Carlo simulation, and machine learning*, volume 133. Springer, 2004.
- [52] Spyridon Samothrakis, Samuel A Roberts, Diego Perez, and Simon M Lucas. Rolling horizon methods for games with continuous states and actions. In *Computational Intelligence and Games (CIG), 2014 IEEE Conference on*, pages 1–8. IEEE, 2014.
- [53] Julian Schrittwieser, Ioannis Antonoglou, Thomas Hubert, Karen Simonyan, Laurent Sifre, Simon Schmitt, Arthur Guez, Edward Lockhart, Demis Hassabis, Thore Graepel, et al. Mastering atari, go, chess and shogi by planning with a learned model. *Nature*, 588(7839):604–609, 2020.
- [54] David Silver, Aja Huang, Chris J Maddison, Arthur Guez, Laurent Sifre, George Van Den Driessche, Julian Schrittwieser, Ioannis Antonoglou, Veda Panneershelvam, Marc Lanctot, et al. Mastering the game of go with deep neural networks and tree search. *nature*, 529(7587):484–489, 2016.
- [55] David Silver, Julian Schrittwieser, Karen Simonyan, Ioannis Antonoglou, Aja Huang, Arthur Guez, Thomas Hubert, Lucas Baker, Matthew Lai, Adrian Bolton, et al. Mastering the game of go without human knowledge. *nature*, 550(7676):354–359, 2017.
- [56] David Silver, Thomas Hubert, Julian Schrittwieser, Ioannis Antonoglou, Matthew Lai, Arthur Guez, Marc Lanctot, Laurent Sifre, Dhharshan Kumaran, Thore Graepel, et al. A general reinforcement learning algorithm that masters chess, shogi, and go through self-play. *Science*, 362(6419):1140–1144, 2018.
- [57] Maciej Świechowski, Tomasz Tajmajer, and Andrzej Janusz. Improving hearthstone ai by combining mcts and supervised learning algorithms. In *2018 IEEE conference on computational intelligence and games (CIG)*, pages 1–8. IEEE, 2018.
- [58] Yunhao Tang and Shipra Agrawal. Discretizing continuous action space for on-policy optimization. In *Proceedings of the aaai conference on artificial intelligence*, volume 34, pages 5981–5988, 2020.
- [59] Yuval Tassa, Tom Erez, and Emanuel Todorov. Synthesis and stabilization of complex behaviors through online trajectory optimization. In *2012 IEEE/RSJ International Conference on Intelligent Robots and Systems*, pages 4906–4913. IEEE, 2012.
- [60] Yuval Tassa, Yotam Doron, Alistair Muldal, Tom Erez, Yazhe Li, Diego de Las Casas, David Budden, Abbas Abdolmaleki, Josh Merel, Andrew Lefrancq, et al. Deepmind control suite. *arXiv preprint arXiv:1801.00690*, 2018.
- [61] Saran Tunyasuvunakool, Alistair Muldal, Yotam Doron, Siqi Liu, Steven Bohez, Josh Merel, Tom Erez, Timothy Lillicrap, Nicolas Heess, and Yuval Tassa. dm\_control: Software and tasks for continuous control. *Software Impacts*, 6:100022, 2020. ISSN 2665-9638. doi: <https://doi.org/10.1016/j.simpa.2020.100022>. URL <https://www.sciencedirect.com/science/article/pii/S2665963820300099>.
- [62] Joe H Ward Jr. Hierarchical grouping to optimize an objective function. *Journal of the American statistical association*, 58(301):236–244, 1963.
- [63] Ari Weinstein and Michael Littman. Open-loop planning in large-scale stochastic domains. In *Proceedings of the AAAI Conference on Artificial Intelligence*, volume 27, pages 1436–1442, 2013.
- [64] Weirui Ye, Shaohuai Liu, Thanard Kurutach, Pieter Abbeel, and Yang Gao. Mastering atari games with limited data. *Advances in Neural Information Processing Systems*, 34:25476–25488, 2021.
- [65] Timothy Yee, Viliam Lisý, and Michael H Bowling. Monte carlo tree search in continuous action spaces with execution uncertainty. In *IJCAI*, pages 690–697, 2016.

## A Potential Negative Societal Impacts

Our work does not appear to have any immediate adverse effects on society. Our research did not involve any human subjects or participants. We only use pre-trained neural network models that have not been trained on sensitive or confidential information. Neither did we use any such information ourselves. Our model does not directly pertain to making real-world decisions involving individuals. However, our work is focused on improving continuous control, which could be applicable to, for instance, robotics. Therefore, it is, in principle, possible that our methods could be employed in unforeseen harmful ways, such as military or law enforcement robotics.

## B Code, Assets, and Reproducibility

The code for reproducing all the main experimental results including the baseline results has been included in the supplementary material zip. The repositories contain the instructions for reproducing the results. The evaluation scripts and the necessary environment files have been included. Due to the size limit, the pre-trained models are not included in the supplementary material: links to download them have been included in the repository READMEs. We used the PlaNet [22] implementation of Arulkumaran [3] and their pre-trained model weights (MIT license).

## C Hyperparameters

Table 3: Experiment-specific hyperparameters of CMCGS.

Parameter	Explanation	Toy Env.	Continuous Control	PlaNet
$N_t$	Trajectories collected in parallel	800	1	400
$ \mathcal{D}_q _{\max}$	Maximum replay buffer size	1000	500	500
$m$	Depth expansion threshold	100	50	50
$\epsilon$	Probability of using node policy $\pi_q$	0.7	0.7	1.0
$N_{\text{top}}$	No. top actions for action selection	50	3	20
$d_{\text{init}}$	Initial depth	5	3	3
$d_{\text{max}}$	Maximum depth	5	$\infty$	10
$N_r$	Rollout length	0	5	5
$n_{\text{max}}$	Maximum number of clusters	2	$\infty$	$\infty$

Table 4: Common hyperparameters of CMCGS.

Parameter	Value
CEM-like elite ratio for updating $\pi_q$ mean	0.1
Inverse-gamma prior distribution for $\pi_q$ variance	$(\alpha = 5, \beta = 1)$
Gaussian noise for top actions	$0.1 \cdot (\mathbf{a}_{\max} - \mathbf{a}_{\min})$

The hyperparameters used for CMCGS are shown in Tables 3 and 4 and included in the submitted code. For the toy environment and continuous control experiments, we have  $\epsilon < 1$ , and when the greedy action is used (see Section 4), it is sampled uniformly from the  $N_{\text{top}}$  best actions. For the PlaNet experiments,  $\epsilon = 1$ , which means that the action is always sampled from  $\pi_q$ . However, the search is conducted with a learned dynamics model. Therefore, the  $N_{\text{top}}$  best actions in the replay buffer of the root node, measured in terms of the trajectory return, are averaged, and the resulting action is taken. The hyperparameters for the baselines have been included in the released code.

For CMCGS, we performed systematic hyperparameter tuning to find the optimum number of trajectories to be collected in parallel for PlaNet and the value of  $\epsilon$  for the continuous control experiments. Smaller-scale experiments were performed to find good values for  $N_{\text{top}}$ ,  $|\mathcal{D}_q|_{\max}$ , and  $N_t$ . Other hyperparameters were not tuned. For MCTS with progressive widening, we performed systematic tuning to find a good value of  $\kappa$  and  $c_{pw}$  that control the number of child nodes allowed, and the constant for the UCB bound. The rollout length was set to be equal to the CMCGS rollout length. For CEM, CMA-ES, and random shooting, we chose the planning horizon to be ten as it is

approximately similar to the planning horizons of MCTS-PW and CMCGS, including the rollouts. Random shooting has no other hyperparameters. For CMA-ES, we used the CMA-ES python library (<https://pypi.org/project/cmaes/>) that has no hyperparameters to be tuned. For the PlaNet experiments, the CEM hyperparameters were copied from the original work [22]. For CEM and continuous control, we tried two different strategies for using the allocated planning budget: keeping the number of trajectories fixed and only modifying the number of iterations, and reducing both the number of trajectories and the number of iterations. We found the latter alternative slightly superior and included that in the paper. The elite ratio of CEM was chosen to be equal to that of CMCGS in the continuous control experiment. All CEM hyperparameters were carefully tuned in the toy environment to extract the best performance.

## **D Infrastructure and Compute**

The toy environment experiments were run on a workstation with a 24-core CPU and 32 GB of memory and took less than 10 minutes. No GPU was used for these experiments. The continuous control and PlaNet experiments were run on an HPC cluster. For evaluating CMCGS with limited environment interaction, we performed  $5 * 10 * 12 = 600$  runs (5 methods, 10 budgets, and 12 environments). Each of these runs used 10 CPU cores with 3 GB of RAM per core. No GPUs were used for these runs. Most runs lasted between one and 24 hours. Some individual runs of MCTS-PW and CMA-ES, especially on the 2d-reacher with a 30-dimensional action space, took between 24 and 72 hours, as these methods were less time efficient on that task. For the PlaNet experiments, we performed  $2 * 20 = 40$  runs (2 methods, 20 seeds, each run evaluated the method on all environments). All runs lasted fewer than 24 hours, and they used one V100 GPU with 32 GB of GDDR SDRAM and 6 CPU workers per GPU.

## E Full Results on Continuous Control with Limited Interaction

### E.1 CMCGS

Table 5: Full results for CMCGS on continuous control with limited interaction: mean plus-minus two standard errors.

Environment	0,5K	1K	1,5K	2K	2,5K	3K
2d-navigation-circles	1.06 ± 0.04	1.11 ± 0.03	1.11 ± 0.03	1.15 ± 0.01	1.15 ± 0.02	1.16 ± 0.01
2d-navigation-boxes	0.30 ± 0.09	0.33 ± 0.09	0.38 ± 0.08	0.53 ± 0.08	0.68 ± 0.07	0.65 ± 0.07
2d-reacher-fifteen-poles	0.31 ± 0.07	0.35 ± 0.07	0.47 ± 0.07	0.43 ± 0.07	0.44 ± 0.07	0.47 ± 0.07
2d-reacher-thirty-poles	0.25 ± 0.06	0.44 ± 0.07	0.41 ± 0.07	0.45 ± 0.07	0.48 ± 0.07	0.45 ± 0.07
ball_in_cup-catch	919.24 ± 12.97	943.47 ± 9.13	956.08 ± 6.09	964.71 ± 5.03	972.01 ± 3.68	971.92 ± 4.33
cartpole-balance_sparse	422.52 ± 41.03	580.78 ± 51.25	695.87 ± 46.79	789.23 ± 45.56	804.29 ± 47.97	873.13 ± 39.85
cartpole-swingup	543.08 ± 14.77	633.23 ± 11.99	712.47 ± 10.97	732.74 ± 10.55	749.54 ± 8.79	762.97 ± 9.36
finger-spin	175.31 ± 6.68	209.90 ± 7.63	247.67 ± 8.14	260.36 ± 9.28	275.52 ± 9.97	274.54 ± 9.22
reacher-hard	743.40 ± 18.95	788.75 ± 15.02	830.67 ± 11.88	867.42 ± 9.14	878.57 ± 9.79	890.55 ± 9.03
cheetah-run	347.73 ± 6.54	394.07 ± 8.74	450.05 ± 8.57	495.30 ± 7.96	522.94 ± 7.81	548.33 ± 8.82
walker-walk	279.06 ± 8.91	294.32 ± 7.42	303.46 ± 7.42	305.23 ± 7.70	307.59 ± 8.37	313.72 ± 6.91
walker-run	105.28 ± 7.03	118.34 ± 7.37	130.76 ± 7.54	143.36 ± 7.11	141.87 ± 8.86	153.50 ± 8.82

Table 6: Full results for CMCGS on continuous control with limited interaction: mean plus-minus two standard errors.

Environment	3,5K	4K	4,5K	5K
2d-navigation-circles	1.12 ± 0.03	1.16 ± 0.01	1.16 ± 0.01	1.17 ± 0.01
2d-navigation-boxes	0.71 ± 0.06	0.75 ± 0.06	0.77 ± 0.06	0.77 ± 0.06
2d-reacher-fifteen-poles	0.51 ± 0.07	0.44 ± 0.07	0.49 ± 0.07	0.45 ± 0.07
2d-reacher-thirty-poles	0.50 ± 0.07	0.53 ± 0.07	0.50 ± 0.07	0.49 ± 0.07
ball_in_cup-catch	973.11 ± 4.04	975.14 ± 3.43	976.24 ± 3.46	976.83 ± 3.12
cartpole-balance_sparse	930.62 ± 30.84	923.17 ± 29.91	970.67 ± 20.56	962.54 ± 22.23
cartpole-swingup	779.99 ± 7.97	785.90 ± 7.23	785.50 ± 7.41	791.67 ± 6.78
finger-spin	284.81 ± 10.85	299.85 ± 10.23	306.31 ± 9.89	299.75 ± 10.78
reacher-hard	900.18 ± 9.43	908.18 ± 7.56	912.32 ± 8.30	912.58 ± 8.58
cheetah-run	565.93 ± 7.17	579.70 ± 7.64	595.04 ± 7.94	601.37 ± 8.15
walker-walk	316.25 ± 7.84	316.18 ± 8.03	318.12 ± 7.40	318.95 ± 7.62
walker-run	158.99 ± 7.62	164.73 ± 8.00	164.20 ± 8.76	167.03 ± 7.66



## E.2 MCTS-PW

Table 7: Full results for MCTS-PW on continuous control with limited interaction: mean plus-minus two standard errors.

Environment	0,5K	1K	1,5K	2K	2,5K	3K
2d-navigation-circles	1.15 ± 0.01	1.16 ± 0.00	1.16 ± 0.00	1.16 ± 0.00	1.16 ± 0.00	1.16 ± 0.00
2d-navigation-boxes	0.23 ± 0.10	0.29 ± 0.09	0.29 ± 0.09	0.38 ± 0.09	0.32 ± 0.09	0.31 ± 0.10
2d-reacher-fifteen-poles	0.12 ± 0.05	0.20 ± 0.06	0.17 ± 0.05	0.15 ± 0.05	0.16 ± 0.05	0.19 ± 0.05
2d-reacher-thirty-poles	0.17 ± 0.05	0.20 ± 0.06	0.19 ± 0.05	0.16 ± 0.05	0.24 ± 0.06	0.22 ± 0.06
ball_in_cup-catch	774.98 ± 54.77	880.36 ± 31.21	894.03 ± 25.10	908.00 ± 29.40	924.13 ± 19.27	921.72 ± 17.42
cartpole-balance_sparse	370.07 ± 37.32	431.52 ± 42.42	497.84 ± 49.39	464.15 ± 44.97	482.74 ± 46.08	428.77 ± 35.91
cartpole-swingup	471.10 ± 13.24	472.97 ± 13.72	478.27 ± 11.79	473.47 ± 11.67	477.44 ± 12.85	469.40 ± 9.97
finger-spin	45.16 ± 4.04	69.23 ± 5.92	95.12 ± 6.23	109.67 ± 7.71	122.69 ± 6.21	129.88 ± 8.35
reacher-hard	700.29 ± 62.17	664.12 ± 69.11	735.29 ± 59.05	749.46 ± 56.43	788.28 ± 51.09	784.26 ± 50.78
cheetah-run	241.09 ± 3.56	273.47 ± 4.61	281.88 ± 5.04	281.93 ± 4.70	288.83 ± 4.86	291.10 ± 5.12
walker-walk	108.60 ± 13.62	134.83 ± 17.06	125.72 ± 14.92	135.88 ± 16.36	150.19 ± 16.90	144.56 ± 15.48
walker-run	45.81 ± 3.82	52.92 ± 5.45	52.72 ± 5.56	53.42 ± 5.44	53.21 ± 5.82	57.25 ± 6.31

17

Table 8: Full results for MCTS-PW on continuous control with limited interaction: mean plus-minus two standard errors.

Environment	3,5K	4K	4,5K	5K
2d-navigation-circles	1.16 ± 0.00	1.16 ± 0.00	1.16 ± 0.00	1.16 ± 0.00
2d-navigation-boxes	0.39 ± 0.09	0.42 ± 0.09	0.42 ± 0.09	0.40 ± 0.09
2d-reacher-fifteen-poles	0.22 ± 0.06	0.14 ± 0.05	0.16 ± 0.05	0.19 ± 0.05
2d-reacher-thirty-poles	0.17 ± 0.05	0.19 ± 0.05	0.25 ± 0.06	0.25 ± 0.06
ball_in_cup-catch	935.72 ± 18.22	945.15 ± 11.90	938.49 ± 15.94	950.63 ± 11.77
cartpole-balance_sparse	502.16 ± 50.72	445.00 ± 37.28	490.06 ± 44.94	493.04 ± 43.65
cartpole-swingup	476.51 ± 12.92	479.66 ± 11.29	477.91 ± 12.89	486.98 ± 14.43
finger-spin	142.34 ± 7.14	152.99 ± 7.75	160.51 ± 8.57	168.08 ± 7.86
reacher-hard	770.08 ± 54.31	777.00 ± 57.73	801.51 ± 46.37	767.84 ± 56.97
cheetah-run	295.62 ± 4.93	297.70 ± 4.95	296.21 ± 5.13	301.34 ± 5.18
walker-walk	146.53 ± 15.72	144.61 ± 16.64	141.71 ± 16.28	143.17 ± 16.19
walker-run	52.63 ± 5.18	58.08 ± 6.40	58.06 ± 6.50	58.14 ± 6.51

### E.3 CEM

Table 9: Full results for CEM on continuous control with limited interaction: mean plus-minus two standard errors.

Environment	0,5K	1K	1,5K	2K	2,5K	3K
2d-navigation-circles	$-0.14 \pm 0.06$	$0.17 \pm 0.04$	$0.27 \pm 0.03$	$0.27 \pm 0.03$	$0.30 \pm 0.03$	$0.29 \pm 0.03$
2d-navigation-boxes	$-0.73 \pm 0.04$	$-0.73 \pm 0.04$	$-0.76 \pm 0.03$	$-0.73 \pm 0.03$	$-0.73 \pm 0.03$	$-0.77 \pm 0.03$
2d-reacher-fifteen-poles	$0.03 \pm 0.02$	$0.07 \pm 0.04$	$0.04 \pm 0.03$	$0.05 \pm 0.03$	$0.05 \pm 0.03$	$0.05 \pm 0.03$
2d-reacher-thirty-poles	$0.06 \pm 0.03$	$0.07 \pm 0.04$	$0.05 \pm 0.03$	$0.06 \pm 0.03$	$0.08 \pm 0.04$	$0.09 \pm 0.04$
ball_in_cup-catch	$330.42 \pm 90.18$	$721.33 \pm 67.67$	$836.54 \pm 46.03$	$865.24 \pm 41.24$	$899.62 \pm 30.61$	$917.54 \pm 22.26$
cartpole-balance_sparse	$575.12 \pm 48.64$	$596.90 \pm 51.68$	$704.00 \pm 51.20$	$758.40 \pm 50.31$	$799.84 \pm 46.29$	$827.84 \pm 42.92$
cartpole-swingup	$620.23 \pm 12.94$	$655.57 \pm 10.27$	$679.89 \pm 11.00$	$676.15 \pm 10.33$	$689.57 \pm 13.04$	$694.91 \pm 13.96$
finger-spin	$22.32 \pm 2.23$	$114.70 \pm 6.78$	$179.08 \pm 8.76$	$207.68 \pm 10.71$	$219.63 \pm 9.42$	$230.14 \pm 9.75$
reacher-hard	$719.92 \pm 59.87$	$774.13 \pm 55.29$	$805.46 \pm 51.66$	$830.10 \pm 42.21$	$853.45 \pm 35.66$	$816.69 \pm 48.26$
cheetah-run	$105.39 \pm 3.81$	$259.85 \pm 4.54$	$321.67 \pm 6.00$	$376.79 \pm 7.42$	$424.01 \pm 9.21$	$459.88 \pm 9.26$
walker-walk	$95.52 \pm 11.00$	$255.65 \pm 15.89$	$292.61 \pm 12.12$	$321.05 \pm 8.00$	$311.47 \pm 7.70$	$316.53 \pm 8.87$
walker-run	$54.21 \pm 3.57$	$89.65 \pm 6.23$	$111.59 \pm 7.50$	$126.72 \pm 8.05$	$134.39 \pm 7.69$	$142.41 \pm 7.91$

Table 10: Full results for CEM on continuous control with limited interaction: mean plus-minus two standard errors.

Environment	3,5K	4K	4,5K	5K
2d-navigation-circles	$0.30 \pm 0.03$	$0.30 \pm 0.03$	$0.27 \pm 0.02$	$0.29 \pm 0.03$
2d-navigation-boxes	$-0.74 \pm 0.03$	$-0.75 \pm 0.03$	$-0.71 \pm 0.04$	$-0.77 \pm 0.03$
2d-reacher-fifteen-poles	$0.07 \pm 0.04$	$0.06 \pm 0.03$	$0.07 \pm 0.04$	$0.14 \pm 0.05$
2d-reacher-thirty-poles	$0.05 \pm 0.03$	$0.08 \pm 0.04$	$0.08 \pm 0.04$	$0.05 \pm 0.03$
ball_in_cup-catch	$918.38 \pm 21.78$	$926.95 \pm 19.82$	$910.18 \pm 26.72$	$941.16 \pm 16.09$
cartpole-balance_sparse	$856.83 \pm 41.43$	$854.63 \pm 41.67$	$837.68 \pm 44.26$	$851.87 \pm 39.71$
cartpole-swingup	$699.89 \pm 15.00$	$720.85 \pm 13.50$	$729.82 \pm 15.09$	$722.87 \pm 15.22$
finger-spin	$237.99 \pm 10.48$	$239.23 \pm 9.39$	$244.84 \pm 10.33$	$242.47 \pm 7.96$
reacher-hard	$866.78 \pm 35.59$	$856.65 \pm 34.60$	$887.47 \pm 26.85$	$865.71 \pm 35.12$
cheetah-run	$492.37 \pm 7.91$	$525.06 \pm 7.90$	$528.55 \pm 8.44$	$543.15 \pm 6.91$
walker-walk	$313.44 \pm 8.63$	$314.85 \pm 7.32$	$314.47 \pm 7.74$	$312.10 \pm 7.37$
walker-run	$142.29 \pm 7.93$	$147.09 \pm 6.90$	$150.20 \pm 7.76$	$151.51 \pm 7.73$

## E.4 Random Shooting

Table 11: Full results for random shooting on continuous control with limited interaction: mean plus-minus two standard errors.

Environment	0,5K	1K	1,5K	2K	2,5K	3K
2d-navigation-circles	0.19 ± 0.04	0.18 ± 0.04	0.17 ± 0.04	0.24 ± 0.04	0.22 ± 0.03	0.21 ± 0.04
2d-navigation-boxes	-0.29 ± 0.05	-0.25 ± 0.05	-0.27 ± 0.05	-0.32 ± 0.05	-0.34 ± 0.05	-0.29 ± 0.05
2d-reacher-fifteen-poles	0.12 ± 0.05	0.09 ± 0.04	0.08 ± 0.04	0.14 ± 0.05	0.05 ± 0.03	0.14 ± 0.05
2d-reacher-thirty-poles	0.09 ± 0.04	0.09 ± 0.04	0.07 ± 0.04	0.09 ± 0.04	0.06 ± 0.03	0.09 ± 0.04
ball_in_cup-catch	937.03 ± 10.02	959.79 ± 5.37	963.08 ± 5.89	968.12 ± 4.21	970.44 ± 4.07	971.61 ± 3.89
cartpole-balance_sparse	464.96 ± 39.98	646.04 ± 45.89	760.54 ± 43.34	856.40 ± 37.06	857.08 ± 38.90	902.18 ± 28.60
cartpole-swingup	595.44 ± 11.95	613.71 ± 11.65	629.75 ± 12.54	645.31 ± 12.55	645.52 ± 12.56	648.04 ± 11.75
finger-spin	160.98 ± 7.12	197.48 ± 8.33	217.34 ± 10.78	232.13 ± 10.20	238.97 ± 8.95	232.79 ± 10.20
reacher-hard	572.72 ± 19.17	645.48 ± 17.13	671.58 ± 16.26	692.90 ± 16.99	711.46 ± 15.86	725.46 ± 14.11
cheetah-run	290.64 ± 6.40	320.53 ± 5.96	341.17 ± 5.98	352.57 ± 5.62	360.96 ± 7.30	367.19 ± 6.70
walker-walk	267.95 ± 6.86	269.58 ± 6.00	279.20 ± 7.40	280.79 ± 7.09	280.45 ± 7.95	279.15 ± 6.26
walker-run	104.97 ± 4.24	112.05 ± 4.57	122.44 ± 4.67	124.62 ± 3.80	128.99 ± 3.81	129.11 ± 3.97

19

Table 12: Full results for random shooting on continuous control with limited interaction: mean plus-minus two standard errors.

Environment	3,5K	4K	4,5K	5K
2d-navigation-circles	0.26 ± 0.04	0.24 ± 0.03	0.25 ± 0.03	0.26 ± 0.03
2d-navigation-boxes	-0.31 ± 0.05	-0.33 ± 0.05	-0.34 ± 0.05	-0.38 ± 0.05
2d-reacher-fifteen-poles	0.11 ± 0.04	0.12 ± 0.05	0.07 ± 0.04	0.08 ± 0.04
2d-reacher-thirty-poles	0.08 ± 0.04	0.12 ± 0.05	0.13 ± 0.05	0.08 ± 0.04
ball_in_cup-catch	973.59 ± 3.49	974.41 ± 3.40	973.34 ± 3.86	974.87 ± 3.36
cartpole-balance_sparse	915.49 ± 27.87	906.85 ± 30.93	951.69 ± 19.80	959.39 ± 19.82
cartpole-swingup	648.48 ± 12.85	660.01 ± 11.86	653.24 ± 12.83	650.19 ± 11.99
finger-spin	230.52 ± 9.85	250.40 ± 10.43	241.56 ± 9.47	245.88 ± 10.29
reacher-hard	725.64 ± 15.54	746.11 ± 13.99	757.15 ± 13.73	756.32 ± 14.23
cheetah-run	371.18 ± 6.65	377.33 ± 8.37	387.32 ± 6.74	383.75 ± 6.82
walker-walk	278.65 ± 6.58	276.61 ± 7.05	272.28 ± 7.49	276.11 ± 7.41
walker-run	131.93 ± 4.46	132.66 ± 4.40	137.39 ± 3.06	140.43 ± 3.87

## E.5 CMA-ES

Table 13: Full results for CMA-ES on continuous control with limited interaction: mean plus-minus two standard errors.

Environment	0,5K	1K	1,5K	2K	2,5K	3K
2d-navigation-circles	$-0.48 \pm 0.06$	$-0.21 \pm 0.06$	$-0.12 \pm 0.06$	$-0.06 \pm 0.06$	$0.00 \pm 0.05$	$0.05 \pm 0.04$
2d-navigation-boxes	$-0.81 \pm 0.04$	$-0.55 \pm 0.06$	$-0.62 \pm 0.05$	$-0.59 \pm 0.05$	$-0.57 \pm 0.06$	$-0.54 \pm 0.05$
2d-reacher-fifteen-poles	$0.08 \pm 0.04$	$0.09 \pm 0.04$	$0.08 \pm 0.04$	$0.08 \pm 0.04$	$0.12 \pm 0.05$	$0.09 \pm 0.04$
2d-reacher-thirty-poles	$0.10 \pm 0.04$	$0.09 \pm 0.04$	$0.08 \pm 0.04$	$0.07 \pm 0.04$	$0.10 \pm 0.04$	$0.09 \pm 0.04$
ball_in_cup-catch	$810.11 \pm 28.83$	$898.36 \pm 15.60$	$924.68 \pm 12.56$	$940.92 \pm 8.41$	$943.71 \pm 10.19$	$946.41 \pm 8.14$
cartpole-balance_sparse	$254.44 \pm 25.05$	$327.53 \pm 29.46$	$368.55 \pm 32.03$	$382.34 \pm 33.94$	$397.54 \pm 36.05$	$430.69 \pm 36.68$
cartpole-swingup	$525.04 \pm 9.08$	$589.20 \pm 8.65$	$618.13 \pm 9.27$	$646.70 \pm 9.64$	$673.50 \pm 12.70$	$696.68 \pm 11.88$
finger-spin	$123.71 \pm 5.88$	$174.48 \pm 7.20$	$201.30 \pm 8.27$	$217.71 \pm 8.55$	$217.13 \pm 9.70$	$230.65 \pm 9.63$
reacher-hard	$478.71 \pm 19.47$	$723.58 \pm 15.48$	$806.71 \pm 13.85$	$849.64 \pm 12.68$	$879.62 \pm 9.41$	$891.60 \pm 10.64$
cheetah-run	$379.54 \pm 12.04$	$511.85 \pm 13.00$	$563.08 \pm 10.13$	$600.29 \pm 11.29$	$621.27 \pm 10.00$	$642.45 \pm 10.89$
walker-walk	$287.32 \pm 8.45$	$321.56 \pm 8.09$	$330.85 \pm 8.80$	$335.09 \pm 8.16$	$344.64 \pm 8.55$	$348.75 \pm 8.29$
walker-run	$122.34 \pm 4.21$	$148.59 \pm 5.14$	$162.94 \pm 6.41$	$173.03 \pm 5.40$	$174.46 \pm 6.84$	$184.43 \pm 5.45$

Table 14: Full results for CMA-ES on continuous control with limited interaction: mean plus-minus two standard errors.

Environment	3,5K	4K	4,5K	5K
2d-navigation-circles	$0.11 \pm 0.05$	$0.12 \pm 0.05$	$0.13 \pm 0.05$	$0.20 \pm 0.04$
2d-navigation-boxes	$-0.56 \pm 0.06$	$-0.56 \pm 0.05$	$-0.43 \pm 0.06$	$-0.48 \pm 0.06$
2d-reacher-fifteen-poles	$0.12 \pm 0.05$	$0.10 \pm 0.04$	$0.06 \pm 0.03$	$0.06 \pm 0.03$
2d-reacher-thirty-poles	$0.09 \pm 0.04$	$0.14 \pm 0.05$	$0.06 \pm 0.03$	$0.12 \pm 0.05$
ball_in_cup-catch	$952.83 \pm 7.85$	$954.25 \pm 8.73$	$959.55 \pm 6.27$	$960.81 \pm 6.76$
cartpole-balance_sparse	$405.10 \pm 34.60$	$437.27 \pm 38.91$	$460.61 \pm 40.94$	$448.40 \pm 38.79$
cartpole-swingup	$695.48 \pm 12.94$	$713.88 \pm 13.50$	$726.56 \pm 13.12$	$733.88 \pm 13.89$
finger-spin	$231.54 \pm 9.04$	$235.70 \pm 7.97$	$242.29 \pm 10.69$	$234.76 \pm 8.77$
reacher-hard	$899.25 \pm 10.09$	$908.92 \pm 8.84$	$905.75 \pm 11.17$	$918.26 \pm 8.74$
cheetah-run	$650.73 \pm 10.05$	$657.26 \pm 9.82$	$678.48 \pm 10.52$	$675.30 \pm 13.50$
walker-walk	$348.28 \pm 8.80$	$353.03 \pm 8.74$	$346.99 \pm 8.01$	$360.31 \pm 9.79$
walker-run	$184.04 \pm 6.34$	$186.70 \pm 6.01$	$188.03 \pm 8.48$	$181.76 \pm 7.76$